PCCP

ARTICLE TYPE

Cite this: DOI: 00.0000/xxxxxxxxxx

Extension and Evaluation of the D4 London Dispersion Model for Periodic Systems

Eike Caldeweyher, Jan-Michael Mewes, Sebastian Ehlert, and Stefan Grimme[a†]

Received Date
Accepted Date

DOI: 00.0000/xxxxxxxxxx

1 SUPPLEMENTARY MATERIAL

1.1 Content

In addition to this PDF, we provide the raw data for all plots shown in this work in the form of a spreadsheet in open-document format (PBE-DATA.ods).

1.2 Theory and implementation

Let us begin with a review of the theoretical framework of the D4 approach[1] as this will provide the context for the introduction of the new features. The underlying concept of D4 and its predecessors is to model the dispersion energy based on atomic pairwise dispersion coefficients C_6^{jk}, which are obtained from a Casimir–Polder integration of the respective atomic polarizabilities $\alpha^{\mathrm{eff}}(i\omega)$

$$C_6^{jk} = \frac{3}{\pi}\int\limits_0^\infty d\omega\, \alpha_j^{\mathrm{eff}}(i\omega)\alpha_k^{\mathrm{eff}}(i\omega). \tag{1}$$

Note that atomic units are used throughout in this work. To account for the influence of the chemical environment, the atomic polarizabilities used in the D4 model are not fixed at the values of the isolated atoms $\alpha(i\omega)$, but depend (i) on geometric parameters captured by the atomic coordination number (CN_j, as in D3), as well as (ii) on effective atomic charges (z_j, new in D4) obtained *via* an electronegativity-equilibration (EEQ) scheme. The idea behind the introduction of this charge scaling is to allow for a more "natural" behavior of the effective polarizabilities, *i.e.*, to render atoms with negative partial charge more polarizable and *vice versa*.

In practice, the geometry and charge dependence of the polarizabilities is implemented using an interpolation based on a set of molecular reference systems. To do this efficiently and avoid an interpolation in two dimensions, the atomic polarizabilities of all reference systems are, in a first step, rescaled to match the effective charge of the atom under consideration of z_j *via*

$$\overline{\alpha}_i^{\mathrm{ref}}(i\omega) = \alpha_i^{\mathrm{ref}}(i\omega)\zeta(z_j, z_i^{\mathrm{ref}}), \tag{2}$$

where ζ describes an empirical relation between the polarizability of an atom and its effective charge. Its analytical form

$$\zeta(z_i, z_i^{\mathrm{ref}}) = \exp\left(\beta\left\{1-\exp\left[\gamma_i\left(1-\frac{z_i^{\mathrm{ref}}}{z_i}\right)\right]\right\}\right), \tag{3}$$

with β as a global parameter set to 3 and γ_i as the chemical hardness taken from Ref. 2 is discussed in more detail in Ref. 1. The calculation of the necessary effective charges z done with an EEQ model is described in section. 1.3

In a second step, the effective polarizability of the atom j is obtained *via* interpolation from the charge-scaled reference polarizabilities using a Gaussian weighting based on the coordination number (CN)

$$\alpha_j^{\mathrm{eff}}(i\omega) = \sum_{i,\mathrm{ref}=1}^{N^{i,\mathrm{ref}}} \overline{\alpha}_i^{\mathrm{ref}}(i\omega)\, W_j^{i,\mathrm{ref}}(\mathrm{CN}_i^{i,\mathrm{ref}}, \mathrm{CN}_j). \tag{4}$$

However, to use this CN-based approach in periodic systems, a different formula for the CN is used compared to the molecular implementation to avoid CN-divergences. The expression for the CN in periodic systems reads

$$\mathrm{CN}_i = \sum_{\mathbf{T}}\sum_{j}{}' \frac{\delta_{ij}^{\mathrm{EN}}}{2}\left(1+\mathrm{erf}\left(-k_0\left(\frac{|\mathbf{R}_{ij}+\mathbf{T}|-R_{ij}^{\mathrm{cov}}}{R_{ij}^{\mathrm{cov}}}\right)\right)\right) \tag{5}$$

$$\delta_{ij}^{\mathrm{EN}} = k_1 \exp\left[-\left(|\mathrm{EN}_i-\mathrm{EN}_j|+k_2\right)^2/k_3\right],$$

where, $\mathbf{T} = t_1\mathbf{a_1} + t_2\mathbf{a_2} + t_3\mathbf{a_3}$ denotes the translation vector with $\mathbf{a_1}$, $\mathbf{a_2}$, and $\mathbf{a_3}$ being the lattice vectors (t_1, t_2, and $t_3 \in \mathbb{Z}$). The primed sum over j indicates that the case $i = j$ is omitted for $\mathbf{T} = \mathbf{0}$. Within the definition of the CN, we apply Pauling elec-

---

[a] *Mulliken Center for Theoretical Chemistry, Mulliken Center for Theoretical Chemistry, Bonn, Germany.*
† E-mail: grimme@thch.uni-bonn.de

tronegativities (EN),[3] as well as the inter-nuclear distance R_{ij} of the pair ij, and the covalent atomic radii[4] ($R_{ij}^{\text{cov}} = R_i^{\text{cov}} + R_j^{\text{cov}}$). Note that the CN has become EN-dependent to differentiate between covalent and ionic bonding (e.g., differentiate F_2 from HF). The parameters in equation 5 ($k_0 = 7.5$, $k_1 = 4.1$, $k_2 = 19.09$, and $k_3 = 254.56$) were taken from Ref. 1.

This charge and geometry dependent calculation of atomic polarizabilities from molecular reference systems, which may be described as an atom-in-molecule approach to polarizabilities, presumes the additivity of atomic polarizabilities,[5] which is reflected in the following equation

$$\alpha_i^{\text{ref}}(i\omega) = \frac{1}{m}\left[\alpha^{I_m X_n}(i\omega) - \frac{n}{l}\,\alpha^{X_l}(i\omega)\zeta(z_X, z_X^{\text{ref}})\right]. \tag{6}$$

Here, $\alpha^{I_m X_n}(i\omega)$ is the molecular polarizability of one I-reference, $\alpha^{X_l}(i\omega)$ refers to the homonuclear compound (e.g., $\alpha^{H_2}(i\omega)$ as dihydrogen) and m, n, and l are the particular stochiometric coefficients. All I atoms inside the reference molecules and the X atoms in the homonuclear compounds are electronically equal and thus symmetry equivalent. By exploiting this symmetry equivalence, the approximation of additive polarizabilities is justified. Furthermore, the charge scaling of all X atoms in the respective reference system is directly incorporated. This more general scheme has no disadvantages compared to the hydrogenated reference systems used in the D3 model. With it, any diatomic molecular polarizabilities, e.g., dihalide molecular polarizabilities (chlorine or fluorine) and oxygen molecular polarizabilities can be used in the subtraction scheme of equation 6 as briefly discussed in Ref. 6. This generalization of the approach opens up the possibility to provide specialized C_6 dispersion coefficients, which is exploited here to properly describe interactions in ionic solids.

1.3 Periodic electronegativity equilibration model

For the generation of atomic partial charges q under periodic boundary conditions, a classical geometry dependent EEQ charge model is developed in the present work. For this purpose, a cyclic cluster model (CCM) is implemented which applies periodic boundary conditions to a cluster that uses a non-primitive unit cell of a solid, a surface, or an infinite chain by directly employing cyclic Born-van-Kármán boundary conditions. The environment of each atom is replaced by a notional cyclic arrangement of cluster atoms, where the interaction zone of each atom within the cyclic cluster is described by a Wigner-Seitz cell, constructed by the translation vectors of the unit cell and centered at the atom. The cluster is constructed as a supercell of the primitive unit cell, so that a repetition of this unit cell of N_1, N_2, and N_3 cells along the lattice vectors $\mathbf{a_1}$, $\mathbf{a_2}$, and $\mathbf{a_3}$ leads to a total cell number of $N = N_1 \cdot N_2 \cdot N_3$. In the CCM, the WSCs are stoichiometrically and symmetrically constructed to ensure local electroneutrality. This is guaranteed by the fact that each WSC central atom i is surrounded by Ξ_i neighbours j with an inverted partial charge. When setting up the cluster, the number of all neighbours of each WSC central atom is determined and weighting factors $w_{ij} = 1/\Xi_i$ for the respective neighbours are assigned, accordingly. Since the CCM is a finite-size method, the clusters used can also carry a net charge without running into convergence problems occurring within the employed Ewald sums. In contrast to a supercell model, no summation over special $\mathbf{k}$-points has to be carried out. Instead, a discrete number of $\mathbf{k}$-points is contained implicitly by placing them equally distributed in space.

$$\{\mathbf{k}\} = \prod_j^3 \frac{g_j}{N_j}\mathbf{b_j} \text{ with } g_j = 0, \ldots, N_j^{-1} \tag{7}$$

Here, we introduce the reciprocal lattice vectors $\mathbf{b}$. The periodic charge density $\rho(r)$ of the system is supposed to be a superposition of spherically symmetric Gaussian functions centered at the atoms position, each normalized to the corresponding nuclear charge q_i given by the following expression

$$\rho_i(r) = \sum_{\mathbf{T}} \frac{q_i}{a_i^3 \pi^{3/2}} \exp\left(-\frac{|\mathbf{r} - \mathbf{R}_i - \mathbf{T}|^2}{a_i^2}\right). \tag{8}$$

Here, the atomic van der Waals radii a_i are introduced. By choosing such atomic charge densities the total isotropic electrostatic (IES) energy is amenable by the following expression given in matrix notation

$$E_{\text{IES}} = \mathbf{q}^T\left(\frac{1}{2}\mathrm{A}\cdot\mathbf{q} - \mathbf{X}\right). \tag{9}$$

The interaction matrix A contains all periodic Coulomb interactions, which are developed in Ewald sums by splitting the Coulomb operator into short-range and long-range contributions (Ewald splitting parameter $\xi = \sqrt{\pi}/V^{1/3}$). Here, the previously determined weighting factors w_{ij} (as obtained from the CCM) are applied for all off-diagonal elements

$$\begin{aligned}
A_{ij}^{\text{rec}} &= \frac{4\pi}{V}\sum_{\mathbf{k}\neq 0}\cos\left(\mathbf{k}\cdot(\mathbf{R}_{ij}+\mathbf{T})\right)\exp\left\{-\frac{k^2}{4\xi^2}\right\}\frac{w_{ij}}{k^2} \\
A_{ii}^{\text{rec}} &= \frac{4\pi}{V}\sum_{\mathbf{k}\neq 0}\exp\left\{-\frac{k^2}{4\xi^2}\right\}\frac{1}{k^2} \\
A_{ij}^{\text{dir}} &= \sum_{\mathbf{T}}\left(\frac{\operatorname{erf}(\gamma_{ij}|\mathbf{R}_{ij}+\mathbf{T}|)}{|\mathbf{R}_{ij}+\mathbf{T}|} - \frac{\operatorname{erf}(\xi|\mathbf{R}_{ij}+\mathbf{T}|)}{|\mathbf{R}_{ij}+\mathbf{T}|}\right)w_{ij} \qquad (10) \\
A_{ii}^{\text{dir}} &= \sum_{\mathbf{T}\neq 0}\frac{\operatorname{erf}(\gamma_{ii}|\mathbf{T}|)}{|\mathbf{T}|} - \frac{\operatorname{erf}(\xi|\mathbf{T}|)}{|\mathbf{T}|} \\
A_{ii}^{\text{self/back}} &= J_{ii} + \frac{2\gamma_{ii}}{\sqrt{\pi}} - \frac{\pi}{\xi^2 V}.
\end{aligned}$$

Furthermore, we define γ_{ij} to be equal to $\left(a_i^2 + a_j^2\right)^{-1/2}$. The Lagrangian is constructed under the constraint that the sum of the atomic charges conserves the total charge of the cluster, *i.e.*,

$$\begin{aligned}
L &= E_{\text{IES}} + \lambda\left(\sum_k q_k - q_{\text{cluster}}\right) \\
&\text{with} \quad \frac{\partial L}{\partial \mathbf{q}} = \mathbf{0} \wedge \frac{\partial L}{\partial \lambda} = \sum_i q_i - q_{\text{cluster}} = 0,
\end{aligned} \tag{11}$$

which leads to a set of $(N+1)$ linear equations. The right-hand side (RHS) of this set of equations is given by $X_i = -\chi_i$, where χ_i

consists of the fitted atomic electronegativity EN_i which is shifted according to the following expression

$$\chi_i = \mathrm{EN}_i - \Omega_i. \tag{12}$$

The molecular EEQ model uses for this shift the square root of a modified error function CN as described in Ref. 1. Since high coordination numbers can be reached very quickly in a periodic system, artificial polarity reversals can occur. An instructive example is displayed in figure 1, where the polarity between cations and anions within the sodium chloride crystal is reversed (*i.e.*, sodium formally becomes anionic and chlorine cationic). This is an artifact of the definition of the CN, which depends on the covalent radius R^{cov} of the respective atom. As a result, the atom with the larger covalent radius also gets a higher CN (here $R^{\mathrm{cov}}_{\mathrm{Na}} = 3.5\,\mathrm{Bohr}$ and $R^{\mathrm{cov}}_{\mathrm{Cl}} = 2.5\,\mathrm{Bohr}$) and thus a higher EN shift resulting in nonphysical polarity changes. In order to avoid such artifacts, the procedure is modified for periodic boundary conditions. Here, Ω_i is used which includes the global parameter $\gamma = 8$ and is given as

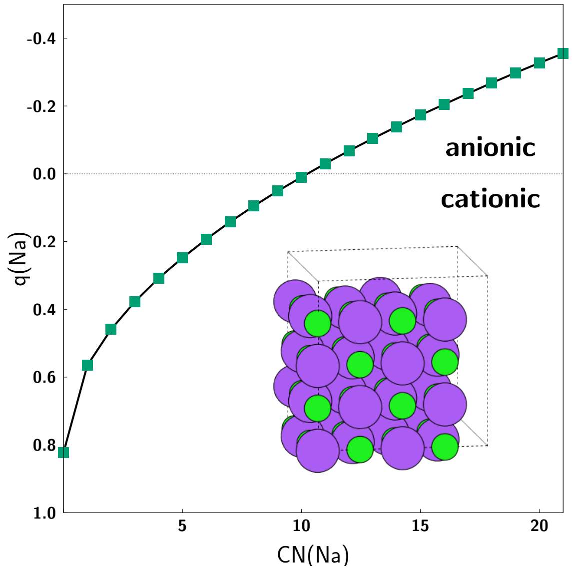

Fig. 1 Functional dependence on the sodium partial charge q(Na) with increasing CN(Na) using the molecular EEQ model within the sodium chloride crystal.

$$\Omega_i = \kappa_i \left(\log \left(\frac{1 + \exp(\gamma)}{1 + \exp(\gamma - CN_i)} \right) \right)^{1/2}. \tag{13}$$

This classical charge model requires overall five empirical parameters (J_{ii}, a_i, EN_i, κ_i, and R^{cov}_i) per element and achieves for molecules across the entire periodic table of elements an average deviation of about 0.04 e^- (0.03 e^- for organic molecules) with respect to PBE0 based Hirshfeld charges.[1]

By using the definition of the Lagrangian given in equation 11 the analytical charge gradients is derived as

$$\frac{\partial \mathbf{q}}{\partial \mathbf{R}_j} = \widetilde{A}^{-1} \left[-\frac{\partial (\mathrm{A} \cdot \mathbf{q})}{\partial \mathbf{R}_j} + \frac{\partial \mathbf{X}}{\partial \mathbf{R}_j} \right] \tag{14}$$

where the inverse of the indefinite $(N+1)$ matrix has been obtained by a Bunch–Kaufman factorization[7] and inversion.

1.4 Dispersion energy

The periodic DFT-D4 energy expression is constructed as follows

$$E^{D4}_{\mathrm{disp}} = E^{(6,8)}_{\mathrm{disp}} + E^{(9),\mathrm{ATM}}_{\mathrm{disp}}. \tag{15}$$

The left part of equation 15 corresponds to the pairwise dispersion energy which is given by

$$E^{(6,8)}_{\mathrm{disp}} = -\frac{1}{2} \sum_i \sum_{\mathbf{T}} \sum_j{}' \sum_{n=6,8} s_n \frac{C^{ij}_{(n)}}{R^{(n)}_{ij_{\mathbf{T}}}} f^{(n)}_{\mathrm{damp}} \left(R_{ij_{\mathbf{T}}} \right). \tag{16}$$

Here, the primed sum over j indicates that the case $i = j$ is omitted for $\mathbf{T} = \mathbf{0}$. In equation 16, s_n scales the individual multipolar contributions—s_6 and s_8 for the dipole–dipole and dipole–quadrupole term—and $f^{(n)}_{\mathrm{damp}}$ denotes the rational Becke–Johnson (BJ) damping function (denoted as BJ-damping (BJD) in the following) which is used to couple this approach to standard DFAs.

$$f^{(n)}_{\mathrm{BJD}}(R_{ij_{\mathbf{T}}}) = \frac{R^{(n)}_{ij_{\mathbf{T}}}}{R^{(n)}_{ij_{\mathbf{T}}} + \left(a_1 R^{ij}_0 + a_2 \right)^{(n)}} \tag{17}$$

Equation 17 incorporates the DFA-specific parameters a_1 and a_2 and the cutoff-radii defined as

$$R^{ij}_0 = \sqrt{\frac{C^{ij}_8}{C^{ij}_6}}, \tag{18}$$

where the recursive relation between dipole–dipole and dipole–quadrupole dispersion coefficients is used. Furthermore, we define the following expression for the rational damping term

$$R^{ij}_{0,\mathrm{BJ}} = \left(a_1 R^{ij}_0 + a_2 \right). \tag{19}$$

The simplest way to include three-body effects uses the well-known Axilrod–Teller–Muto[8,9] (ATM) term (*cf.*, right side of equation 15) which is defined as the sum over ijk energy contributions each defined by

$$E^{ijk} = \frac{C^{ijk}_9 \left(3\cos\theta_i \cos\theta_j \cos\theta_k + 1 \right)}{\left(R_{ij} R_{jk} R_{ki} \right)^3}. \tag{20}$$

Here, θ_i, θ_j, and θ_k are the internal angles of the triangle formed by R_{ij}, R_{jk}, and R_{ki} while C^{ijk}_9 is the triple-dipole constant given by

$$C^{ijk}_9 \approx \sqrt{C^{ij}_6 C^{jk}_6 C^{ki}_6}. \tag{21}$$

The C^{ijk}_9 coefficients are derived from C_6 coefficients which are obtained from charge-neutral atomic polarizabilities (i.e., neutral atoms with $z_i = Z_i$). The finally used three-body dispersion energy expression is as follows

$$\begin{aligned} E^{(9),\mathrm{ATM}}_{\mathrm{disp}} &= \\ &- k \sum_i \sum_{\mathbf{T}} \sum_j \sum_{\mathbf{T}'}{}' \sum_k{}'' f^{(9)}_{damp}(\overline{R}_{ij_{\mathbf{T}}k_{\mathbf{T}'}}) E^{ij_{\mathbf{T}}k_{\mathbf{T}'}}, \end{aligned} \tag{22}$$

where the sum is over all atom triples ijk applied with a zero-damping scheme proposed by Chai and Head-Gordon[10]

$$f^{(9)}_{damp}(\overline{R}_{ij_{\mathbf{T}}k_{\mathbf{T}'}}) = \frac{1}{1+6\left(\overline{R}_{ij_{\mathbf{T}}k_{\mathbf{T}'}}\right)^{-16}}. \tag{23}$$

To avoid multiple counting of three-body interactions the factor k is set to $\frac{1}{3}$ if atoms i, j, k are within the reference cell and to $\frac{1}{2}$ in all other cases. As previously, the primed sum over j indicates that the case $i = j$ is omitted for $\mathbf{T} = \mathbf{0}$, the double primed sum over k indicates that the case $j = k$ is omitted for $\mathbf{T} = \mathbf{T}'$ and $i = k$ is omitted for $\mathbf{T} = \mathbf{0}$. Equation 23 includes the averaged inter-atomic distance

$$\overline{R}_{ij_{\mathbf{T}}k_{\mathbf{T}'}} = \left(R_{ij_{\mathbf{T}}}\,R_{j_{\mathbf{T}}k_{\mathbf{T}'}}\,R_{k_{\mathbf{T}'}i} \Big/ R^{ij}_{0,\mathrm{BJ}}R^{jk}_{0,\mathrm{BJ}}R^{ki}_{0,\mathrm{BJ}}\right)^{1/3}, \tag{24}$$

which incorporates $R^{ij/jk/ki}_{0,\mathrm{BJ}}$ (*cf.* equation 19). Since dispersion interactions are much faster decaying (leading order term $\propto R^{-6}$) than, e.g., Coulomb interactions we employ for this energy contribution a real-space cutoff within the periodic implementation. Furthermore, analytical gradients are available for the dispersion energy expression in equation 15.

1.5 Theory of the Quasi-harmonic approximation

In order to account for thermodynamic properties to crystals, the knowledge of phonon modes is required over the complete first Brillouin zone (FBZ) of the system. The easiest way to account for ZPVE contributions includes harmonic lattice dynamics where each **k**-point in the FBZ is associated with 3M harmonic oscillators (*i. e.* phonons) which are labeled by a phonon band index n ($n = 1,\ldots,3N$) and whose energy levels are given by the usual harmonic expression as

$$\varepsilon^{n,\mathbf{k}}_m = \left(m+\frac{1}{2}\right)\omega_{\mathbf{k}n}, \tag{25}$$

where m is an integer, $\omega_{\mathbf{k}n} = 2\pi\nu_{\mathbf{k}n}$, and N is the number of atoms per primitive cell. The overall vibrational canonical partition function of a crystal at a given temperature T is given as

$$Q_{vib}(T) = \prod_{\mathbf{k}}\prod_{n=1}^{3N}\sum_{m=0}^{\infty}\exp\left(-\frac{\varepsilon^{n,\mathbf{k}}_m}{k_BT}\right), \tag{26}$$

where k_B is Boltzmann's constant. From this expression it is straightforward to obtain harmonic expressions to the internal energy given as

$$\mathscr{E}(T) = k_BT^2\left(\frac{\partial\log(Q_{vib})}{\partial T}\right) = \sum_{\mathbf{k}n}\hbar\omega_{\mathbf{k}n}\left(\frac{1}{2}+\frac{1}{\exp\left(\frac{\hbar\omega_{\mathbf{k}n}}{k_BT}\right)-1}\right). \tag{27}$$

However, the harmonic approximation has its limitations like zero thermal expansion, temperature independence of elastic constants and bulk modulus, equality of constant-pressure and constant-volume specific heats, as well as infinite thermal conductivity and phonon lifetimes.[11] To overcome such drawbacks, the simplest way includes quasi-harmonic quantities in the sense of the quasi-harmonic approximation (QHA).[12–15] According to the QHA the Helmholz free energy of a crystal is written retaining the same harmonic expression but introducing an explicit dependence of vibrational phonon frequencies on volume as given by

$$F^{QHA}(T,V) = U_0(V) + F^{QHA}_{vib}(T,V), \tag{28}$$

where $U_0(V)$ is the zero-temperature internal energy of the crystal without any vibrational contribution (similar to volume constrained geometry optimizations) and the vibrational part is given by

$$F^{QHA}_{vib}(T,V) = \sum_{\mathbf{k}n}\frac{\hbar\omega_{\mathbf{k}n}(V)}{2} + k_BT\left[\ln\left(1-\exp\left(-\frac{\hbar\omega_{\mathbf{k}n}(V)}{k_BT}\right)\right)\right], \tag{29}$$

where the first part refers to the zero-point energy of the system. The equilibrium volume at a given temperature T is obtained by minimizing $F^{QHA}(T,V)$ with respect to volume V while keeping T constant.

1.6 Technical details

All molecular dynamic dipole polarizabilities $\alpha(i\omega)$ were calculated using time-dependent density functional theory (TD-DFT).[16,17] A variant of the PBE0 hybrid functional was used, with a Fock-exchange admixture of 37.5% (dubbed PBE38). This method has already proved its accuracy and robustness in previous works.[1,18,19] The atomic orbital (AO) basis sets used in the TD-DFT calculations are of def2-QZVP[20,21] quality closely representing the complete basis set (CBS) limit for this property. The following ECPs are used: ecp-2-sdf (unpublished, Stuttgart group) covering 2 core electrons, ecp-10-sdf (unpublished, Stuttgart group) covering 10 core electrons, ecp-18-sdf (unpublished, Stuttgart group) covering 18 core electrons, ecp-36-sdf (unpublished, Stuttgart group) covering 36 core electrons, ecp-54-sdf (unpublished, Stuttgart group) covering 54 core electrons, ECP-28[22–24] covering 28 core electrons (for Rb, Sr, Y-Cd, In-SB, Te-Xe, Ce-Lu), ECP-46 covering 46 core electrons (for Cs, Ba, La), and ECP-60 covering 60 core electrons (for Hf-Hg, Tl-Bi, Po-Rn) as defined in Ref. 20. Crystal structures have been extracted from MATERIALS PROJECT[25] (for alkali metals Li, Na, K, Rb, and Cs; for alkaline earth metals Be, Mg, Ca, Sr, and Ba; for *d*-block elements Sc and Y) and used within the PEECM to obtain dynamic polarizabilities. Since some elements have experimental crystal structures that exhibit high dipole moments, the PEECM calculation could not be successfully converge (e.g, for Ti, Zr, Hf, V, Nb, and Ta). For these elements closed-shell monomers without dipole moments were extracted from the crystal structure and dynamic polarizabilities were calculated using the presented level of theory. Furthermore, periodic coordination numbers were assigned to those six extracted clusters to be used as approximated "periodic" reference system. The ECPs used to create the shells within part (II) of the particular clusters have been extracted from the TURBOMOLE[26,27] basis set library (nomenclature reads as follows element/ecp-electrons in core-name; for alkali metals we used: Li/ecp-2-sdf, Na/ecp-10-sdf, K/ecp-18-sdf, Rb/ecp-36-sdf, and Cs/ecp-54-sdf; for earth alkali metals we used: Be/ecp-2-sdf, Mg/ecp-10-sdf[28], Ca/ecp-18-sdf, Sr/ecp-36-sdf, and Ba/ecp-54-

sdf; for d-block elements we used: Sc/ecp-10-mdf[29], Y/ecp-28-mwb[22]; for halogen we applied Cl/ecp-10-sdf and F/ecp-2-sdf and for oxygen we applied O/ecp-2-sdf).

1.7 Computational details

1.7.0.1 BJ-damping parameter For consistency we add the BJ-damping parameter that are used in this work.

Table 1 Applied BJ-damping parameter of different DFAs as extracted from Ref. 1.

DFA	s_6	s_8	a_1	a_2
PW91	1.0000	0.77283111	0.39581542	4.93405761
SCAN	1.0000	1.46126056	0.62930855	6.31284039
PBE	1.0000	0.95948085	0.38574991	4.80688534
RPBE	1.0000	1.31183787	0.46169493	3.15711757
revPBE	1.0000	1.74676530	0.53634900	3.07261485
BLYP	1.0000	2.34076671	0.44488865	4.09330090
B3LYP	1.0000	2.02929367	0.40868035	4.53807137
TPSS	1.0000	1.76596355	0.42822303	4.54257102
PBE0	1.0000	1.20065498	0.40085597	5.02928789
revPBE	1.0000	1.74676530	0.53634900	3.07261485

1.7.0.2 X23: Solid state volumina For the determination of the 23 molecular crystal structure volumes we applied the VASP 6.0.8 software package. All PBE PAW calculations used an 800eV plane-wave cutoff (convergence criteria: energy difference $\propto 10^{-6}$). The DFT conjugated gradient method has been used within the optimization where all atomic positions and the cell has been relaxed. For all calculations standard pseudopotentials have been used.

1.7.0.3 ICE10: QHA calculations Quasi-harmonic approximation calculations have been performed for eight different ice polymorphs. For this purpose the QHA implementation within the CRYSTAL17 code has been applied in combination with HSE-3c. Here, four different volumina have been used (steps of 2.5%) for which overall ten different temperatures have been applied (ranging from 10 K to 100 K applying 10 K steps). V_0 has been extracted from Helmholtz free energy calculations at a pressure of 0 GPa.

1.7.0.4 Timings for the cyclohexanedione crystal A self-consistent field (SCF) calculation has been performed for the clohexanedione crystal using the PBE/800eV setup in VASP 6.0.8 (convergence criteria: energy difference $\propto 10^{-6}$). The converged wave function has been applied to determine the pure timing arising from each dispersion correction. For SCAN-rVV10 and vdW-DF2 we applied an PAW cutoff of 800eV. For all calculations standard pseudopotentials have been used.

1.7.0.5 Salt polarizabilities Salt polarizabilities have been calculated for several alkali halides. For D3 and D4 we use polarizabilities from the DFTD3 and DFTD4 standalone programs. For other dispersion corrections we have calculated polarizabilities using VASP 6.0.8 with a PBE/800eV setup using standard pseudopotentials.

2 References

Notes and references

1 E. Caldeweyher, S. Ehlert, A. Hansen, H. Neugebauer, S. Spicher, C. Bannwarth and S. Grimme, *J. Chem. Phys*, 2019, **150**, 154122.

2 D. C. Ghosh and N. Islam, *Int. J. Quantum Chem.*, 2010, **110**, 1206–1213.

3 L. Pauling, *Cornell University, Press, Ithaca, New York*, 1960, 17.

4 P. Pyykkö and M. Atsumi, *Chem.-Eur. J.*, 2009, **15**, 186–197.

5 K. J. Miller, *J. Am. Chem. Soc.*, 1990, **112**, 8533–8542.

6 S. Ehrlich, J. Moellmann, W. Reckien, T. Bredow and S. Grimme, *ChemPhysChem*, 2011, **12**, 3414–3420.

7 J. R. Bunch and L. Kaufman, *Linear Algebra Its Appl.*, 1980, **34**, 341–370.

8 B. M. Axilrod and E. Teller, *J. Chem. Phys.*, 1943, **11**, 299–300.

9 Y. Muto, Proc. Phys. Math. Soc. Jpn., 1943, pp. 629–631.

10 J.-D. Chai and M. Head-Gordon, *Phys. Chem. Chem. Phys.*, 2000, **10**, 6615–6620.

11 M. T. Dove, *Introduction to lattice dynamics*, Cambridge university press, 1993, vol. 4.

12 A. Erba, *J. Chem. .Phys.*, 2014, **141**, 124115.

13 A. Erba, M. Shahrokhi, R. Moradian and R. Dovesi, *J. Chem. Phys.*, 2015, **142**, 044114.

14 A. Erba, J. Maul, M. De La Pierre and R. Dovesi, *J. Chem. Phys.*, 2015, **142**, 204502.

15 A. Erba, J. Maul, M. Itou, R. Dovesi and Y. Sakurai, *Phys. Rev. Lett.*, 2015, **115**, 117402.

16 S. J. A. van Gisbergen, J. G. Snijders and E. J. Baerends, *J. Chem. Phys.*, 1995, **103**, 9347–9354.

17 V. P. Osinga, S. J. A. van Gisbergen, J. G. Snijders and E. J. Baerends, *J. Chem. Phys.*, 1997, **106**, 5091–5101.

18 S. Grimme, J. Antony, S. Ehrlich and H. Krieg, *J. Chem. Phys.*, 2010, **132**, 154104.

19 E. Caldeweyher, C. Bannwarth and S. Grimme, *J .Chem. Phys.*, 2017, **147**, 034112.

20 F. Weigend and R. Ahlrichs, *Phys. Chem. Chem. Phys.*, 2005, **7**, 3297–3305.

21 F. Weigend, F. Furche and R. Ahlrichs, *J. Chem. Phys.*, 2003, **119**, 12753–12762.

22 D. Andrae, U. Haeussermann, M. Dolg, H. Stoll and H. Preuss, *Theor. Chem. Acc.*, 1990, **77**, 123–141.

23 B. Metz, H. Stoll and M. Dolg, *J. Chem. Phys.*, 2000, **113**, 2563–2569.

24 K. A. Peterson, D. Figgen, E. Goll, H. Stoll and M. Dolg, *J. Chem. Phys.*, 2003, **119**, 11113–11123.

25 A. Jain, S. P. Ong, G. Hautier, W. Chen, W. D. Richards, S. Dacek, S. Cholia, D. Gunter, D. Skinner, G. Ceder and K. A. Persson, *APL Materials*, 2013, **1**, 011002.

26 F. Furche, R. Ahlrichs, C. Hättig, W. Klopper, M. Sierka and F. Weigend, *WIREs Comput. Mol. Sci.*, 2014, **4**, 91–100.

27 R. Ahlrichs, M. Bär, M. Häser, H. Horn and C. Kölmel, *Chem.*

Phys. Lett., 1989, **162**, 165–169.

28 P. Fuentealba, L. Von Szentpaly, H. Preuss and H. Stoll, *Journal of Physics B: Atomic and Molecular Physics*, 1985, **18**, 1287.

29 M. Dolg, U. Wedig, H. Stoll and H. Preuss, *J. Chem. Phys.*, 1987, **86**, 866–872.